

Optimization methods for complex sheet metal stamping computer aided engineering

Giuseppe Ingarao · Rosa Di Lorenzo

Received: 15 April 2010 / Revised: 4 May 2010 / Accepted: 12 May 2010 / Published online: 29 May 2010
© Springer-Verlag 2010

Abstract Nowadays, sheet metal stamping processes design is not a trivial task due to the complex issues to be taken into account (complex shapes forming, conflicting design goals and so on). Therefore, proper design methodologies to reduce times and costs have to be developed mostly based on computer aided procedures. In this paper, a computer aided approach is proposed with the aim to offer a methodology able to solve very complex sheet metal stamping processes, in particular a progressive design approach based on the integration between numerical simulations and optimization methodologies is presented. In particular, Response Surface Method, Moving Least Squares approximation and Pareto optimal solutions search techniques were applied in order to design two different complex 3D stamping operations. The proposed design procedure is able to verify the necessity of a spatially differentiated restraining forces approach and to design the best policy for them. In particular, different part “quality” indicators were monitored such as springback occurrence and thinning. An explicit/forming-implicit/springback approach was utilized to develop the numerical simulations. To sum up, a new and flexible design methodology is proposed, able to: deal with complex sheet metal stamping processes; investigate many possible technological scenarios; carry out a set of reliable solutions able to satisfy different design requirements; offer different optimization possibilities in order to take in to account all the sheet metal stamping design issues.

Keywords Sheet stamping · Response surface methodology · Moving least squares approximation · Restraining forces

1 Introduction

Sheet metal forming is, nowadays, one of the most important manufacturing technology, and it is worth pointing out that the growing interest in this technology led, in the latest years, to the request of very complex shapes. As a consequence, the design of the sheet metal stamping processes became very difficult to set up, since the design variables number is progressively increased. Even if the numerical simulation has strongly reduced the design costs and times, the growing number of design parameters makes the implementation of intelligent optimization techniques necessary in order to reduce the number of numerical simulations to be run.

When complex sheet stamping processes are designed, three main topics have to be taken into account:

- Design goals;
- Operative parameters control to achieve design goals;
- Methodologies for the design process.

1.1 Sheet stamping design goals

When goals of a sheet stamping process design are considered, different topics have to be considered: formability, defects, lightweight materials just to refer to the most investigated ones. As defects are regarded, two main categories may be classified: thinning related ones (fractures, wrinkling, thickening etc.) and dimensional errors (mainly related to springback distortions). The increasing role of

G. Ingarao · R. Di Lorenzo (✉)
Dipartimento di Tecnologia Meccanica, Produzione e Ingegneria
Gestionale, Università di Palermo, Palermo, Italy
e-mail: rosanna@dtpm.unipa.it

lightweight manufacturing led to the success of materials such as advanced high strength steels (AHSS, as TRIP or DP steels), and light weight alloys (magnesium and aluminium alloys). The main research issues related to such materials are formability and springback. Nowadays, in a complex 3D industrial forming processes design, the total compensation (or at least reduction or control) of the springback distortions is a crucial issue since it implies a minimization of reworking costs. It should be observed that, after a stamping operation, springback occurs since, as the forming tools are removed, the residual internal stress state of the component is not equilibrated by the external actions of the tools anymore and an elastic deformation occurs, leading to a new geometry for which the residual internal stress state is self equilibrated. The inhomogeneous strains distribution along the stamped sheet thickness, together with the elastic–plastic behaviour of the workpiece material, determines springback.

Nowadays, springback analysis strongly depends on numerical capabilities: it is well known that numerical simulation of elastic springback phenomenon is not as effective and reliable as the forming process one. For these reasons, the investigation of finite element formulations aimed to analyze and predict springback effects have become very attractive also due to the rapid increase in computational power. Many approaches to simulate springback have been recently proposed, including explicit–explicit, static explicit–static explicit, and even one step method (Li et al. 2002). Many numerical parameters influence springback prediction accuracy: the utilized element, the number of integration points, the shape and the evolution of the yield surface (Xu et al. 2004; Wagoner and Li 2007; Geng and Wagoner 2004a, b). Several research groups analyzed the effects of tools geometry and of process parameters (such as friction conditions, blank holder forces, punch and die radius and so on) on springback predictions with FEA (Pepelux and Ponthot 2002). Nowadays, some papers are focused on integration between optimization techniques and numerical simulations in order to control, predict and minimize springback amount in sheet metal forming operations. Some researches focused on die compensation methodologies (Geng and Wagoner 2004a, b; Cheng et al. 2007) while other researchers utilized the integration between RSM and finite element methods (FEM) in order to find out both process and material parameters for springback minimization (Naceur et al. 2006, 2008). Also intelligent techniques, such as Artificial Neural Networks, were utilized to predict springback in wipe-bending process (Kazan et al. 2009). As thinning related defects are concerned, they have been widely investigated in the technical literature and they are strictly related to formability issues. The utilisation of FLDs is commonly recognised as a very effective tool to investigate failure. Nevertheless, the state of the art in this research

field assesses that FLDs do not perform well if non-linear strain paths are concerned (Wu et al. 2005). Moreover, the FLDs utilisation can be considered a qualitative tool to predict fracture in particular if complex stamping operations are taken into account. On the other hand, the utilisation of forming limit stress diagrams (Uthaisangsuk et al. 2007) is considered a good tool to represent fracture limits but such diagrams need to be properly tuned to derive a proper indicator of fracture risk. In an industrial environment a quick and simple fracture indicator is the maximum thinning (Shivpuri and Zhang 2009). Moreover, thinning distribution allows also the control of wrinkling (which could be evidenced by eventual thickening) if it is necessary.

1.2 Sheet stamping design operative parameters

In the latest years, many researches focused on the integration between numerical simulations and optimization techniques in order to optimize sheet metal stamping process parameters (Hu et al. 2008): initial blank shape, blank holder force, draw beads penetration and so on. Moreover, the complexity of stamped component shapes makes the implementation of a differentiated restraining force approach strictly necessary. A localized control of the material flow into the dies is often required in order to locally induce (or eventually avoid) stretching phenomena. A methodology to differentiate restraining forces is the segmented blank holder utilization (Lin et al. 2007). Some authors (Wang and Lee 2005) presented the integration between numerical simulations and Response Surface Methodology (RSM) to optimize the action of a segmented blank holder in a rectangular box deep drawing; in particular, the restraining forces are modelled by two blank holder forces and by friction coefficient. Shivpuri and Zhang (2009), investigated the optimal design of spatially varying frictional constraints for reducing both the risk of wrinkling and excessive thinning: a strong improvement with respect to the spatially uniform friction case was demonstrated. Another strategy to spatially differentiate the restraining forces is related to the utilization of some draw beads characterized by different penetration values (Jansson et al. 2005a, b). Another research (Breitkopf et al. 2005) focused on the utilization of response surface methodology to optimize sheet metal forming process: an approximation based on moving least squares is proposed in order to reduce the total number of the numerical simulations to be run. Donglai et al. (2008) optimize three different draw beads and a blank holder force value to minimize wrinkling tendency, checking also excessive thinning and insufficient stretching.

It is important to underline the linkage between a spatially differentiated restraining forces approach and the control the springback amount. Springback minimization

strongly depends on process mechanics over the sheet during the stamping processes: increasing stretching mechanics would be useful in reducing springback. As a consequence, thinning tendency unavoidably increases too. Therefore, springback minimization problems are typically multi-objective ones for which a proper restraining forces policy has to be calibrated.

1.3 Sheet stamping design methodologies

Sheet stamping design problems are generally multi-objective ones and usually require multi-objectives optimisation techniques. Nevertheless, the solutions to such problems may, in some cases, derive also from the application of mono-objective approaches. Actually, if a complex sheet stamping process is investigated, there is the possibility to analyse it under particular hypotheses which allow the application of mono-objectives optimisation approaches.

When multi-objective optimisation problems are developed within a sheet metal stamping design, some crucial issues to be taken into account:

- Multi-objective problems are generally characterized by conflicting objectives;
- In most of the metal forming operations optimization problems the analytical linkages between the design variables and the objective functions are not available;
- In an industrial environment a great interest would be focused on the availability of a cluster of possible optimal solutions instead of a single “almost optimal” solution.

Some multi-objective techniques have been presented with applications in sheet metal stamping optimization. Some authors used a multi-objective genetics algorithm to design blank-holding force and draw-bead restraining force in an auto-body panel stamping process aiming to optimize, simultaneously, four different objective functions (fracture, wrinkling, stretching and thickness variation) (Wei and Yuying 2008). Other authors utilized a surrogate response surface method for the design of a deep drawing operation on aluminium parts (Zhang and Shivpuri 2009). Another research is focused on the optimal design of varying frictional constraints to reduce the risk of failure due to wrinkling and thinning (Shivpuri and Zhang 2009). Some works are focused on the optimal design of forming operations based on the integration between finite element analysis (FEA) and a multi-objective genetic algorithm (MOGA) (Wei and Yuying 2007). Some authors (Liu et al. 2008) propose a novel multi-objective approach applied on a sheet metal stamping process: in particular, the blank holder force path is considered as design parameter and cracking and

wrinkling are selected as two objectives of this optimization problem. Finally, a first attempt of simultaneous control of springback and thinning distribution utilizing multi-objective genetic algorithm was developed by Wei et al. (2009). The authors have experienced the multi-objective approaches usefulness on sheet metal stamping operations design (Ingarao et al. 2009a, b). It is worth pointing out that, for particular case studies, the knowledge available on the process and the specific design requirements may avoid a multi-objective formulation of the design problem: the problem remains a multi-objective one but its optimisation may be performed by a classical mono-objective minimization. In these cases, the final desired solution may be reached applying a mono-objective approach. Regarding such problems, in metal forming optimisation, several approaches were developed (Meinders et al. 2008). Some approaches are characterised by a certain number of iterations of an iterative algorithm (usually gradient based) which are stopped when convergence is reached. Generally, such algorithms are interfaced with numerical simulation aimed to solve a certain number of direct problems necessary to calculate objective function gradients. Such algorithms may lead to local minima instead of global ones even if many of these algorithms are very efficient since few iterations are necessary to reach technologically satisfying results (Fann and Hsiao 2003; Kleinermann and Ponthot 2003; Naceur et al. 2004; Zhao et al. 2004). The authors experienced the application of gradient based algorithms on a decomposition domain approach and on a cascade optimization methodology, both the applications aimed to optimize an Y-shaped tube hydroforming process (Di Lorenzo et al. 2009, 2010). A different approach is based on intelligent techniques, for instance, genetic algorithms found a lot of applications (Schenk and Hillmann 2004; Fourment et al. 2005; Castro et al. 2004) even if they, generally, require a high number of objective function evaluations. Some authors presented also some approaches which are based on the possibility to adapt the finite element analysis by some proper adaptive algorithms aimed to optimise some time dependent variables of a given process along the numerical simulations: of course, such approaches imply the possibility to manage the source code of a finite element software (Jansson et al. 2007; Sheng et al. 2004). Maybe, one of the most effective approach presented in the recent years in the technical literature is founded on response surface methodology (Myers and Montgomery 2002). Response surface methods (RSM) are based on approximation of a given objective function to be optimised through a set of points belonging to the domain of variation of the independent variables the function itself depends on. Some works are focused on the application of RSM in sheet metal forming aimed to reduce the number of numerical simulations (Breitkopf et al. 2005; Jansson et al. 2005a, b; Naceur et al. 2006):

some authors used surrogate models and response surfaces in order to optimise a stamping operation for an automotive component (Jansson et al. 2005a, b) while other authors focused on springback effects control through RSM based approaches (Naceur et al. 2006).

A very interesting aspect in RSM application regards the possibility to build response surfaces basing on moving least squares approximations (MLS) by utilising a moving region of interest (Breitkopf et al. 2005; Oudjene et al. 2009). MLS are commonly used in mesh free methods as well as in many computational mechanics applications (Belytschko et al. 1996; Rassineux et al. 2003; Breitkopf et al. 2004). The MLS approach was also utilised in metal forming problems such as in optimising complex stamping operation even for industrial automotive cases (Breitkopf et al. 2005; Naceur et al. 2006).

1.4 Paper contribution

It is well recognised that a computer aided sheet metal stamping design tool is crucial to reduce design times and costs. In particular, in the field of computer aided design approaches any sheet stamping optimization tool has to take into account the following fundamental aspects:

- A policy based on spatially differentiated restraining forces has to be taken into account;
- Springback has to be controlled as stamped part quality indicator;
- A multi-objective approach could be very useful to support the designer decisions;
- An optimization procedure has to include the possibility to obtain an optimal solution with low computational effort.

In this paper, a methodology able to take into account all the mentioned issues is proposed. The main aim of the research is to offer a procedure able to solve very complex sheet metal stamping design problems: a progressive design approach based on the integration of numerical simulations with optimization methodologies is presented. Response Surface Method (RSM), Moving Least Squares (MLS) approximation and Pareto optimal solutions search techniques were applied in order to design two different complex 3D stamping operations. Thickness control and springback distortions were taken in to account as stamped part quality indicators.

The proposed design methodology is based on a former decision step leading to a Pareto front under the hypothesis of uniform restraining forces application. The following step may developed along two scenarios: a multi-objective approach or instead a mono-objective one.

Moreover, as the mono-objective optimization is concerned, an innovative procedure is presented based on the application of a progressive MLS. The final aim of the paper is the assessment of a new and flexible design methodology, able to:

1. Solve complex sheet metal stamping processes design problems;
2. Investigate many possible technological scenarios;
3. Carry out a set of reliable solutions able to satisfy different design requirements;
4. Develop an optimization procedure able to offer satisfying solutions with a very few number of design variables;
5. Offer two different optimization possibilities in order to take in to account all the sheet metal stamping design issues.

2 Design strategy

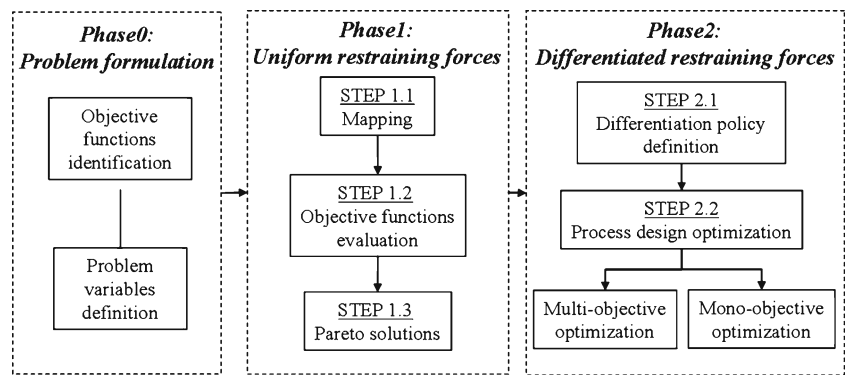
As already mentioned, one of the main issue related to complex sheet metal stamping processes design, concerns the best restraining forces policy. The proposed methodology is based on Pareto optimality and enables both to understand if a differentiated restraining forces approach is necessary and which is the best restraining forces policy. When a complex sheet metal stamping process is designed an early process engineering is always requested in order to achieve a deep knowledge of the process mechanics. Moreover, if a uniform restraining force policy leads to good results in terms of design requirements, the necessity to differentiate maybe avoided with consequent lessen of time and tooling costs (a segmented blank holder, for instance, may represent a cost increase). An initial analysis using uniform restraining forces is necessary to build up of a sort of benchmark to evaluate the subsequent differentiated restraining forces policy results.

The proposed methodology is modelled and summarized in Fig. 1; the different phases are detailed in the following sections.

2.1 Phase 0

This former phase is the so-called modelling phase: proper design variables to be optimised have to be chosen and objective functions have to be defined. The most relevant parameters for process design have to be chosen as design variables the objective function and the constraint functions depend on. For a given optimization problem, a design variables vector can be written as: $\mathbf{x} = [x_1, x_2, \dots, x_N]$ (N indicates the total number of variables, such number should be kept as small as possible).

Fig. 1 The proposed design procedure



Objective functions ($f(x)$) express specific design intentions that need to be minimized (or maximized). In other words, an objective function is a performance (“quality”) measure of whatever the design problem intends to optimize. Objective functions may be explicit or implicit in (x) and may be evaluated by analytical or numerical techniques (i.e. FE simulations). Once the analyzed process is modelled in terms of design variables and objective functions, integration between numerical simulation and an optimization algorithms is necessary to update the design variables values towards the objective functions minimisation.

2.2 Phase 1

As it can be observed the procedure consists of two essential domains: the former refers to uniform restraining forces policy while the latter concerns a differentiated restraining forces approach. The former policy is focused on a preliminary mapping step (step 1.1) at the varying of the blank holder force and it is necessary in order to evaluate (step 1.2) critical regions in terms, for instance, of fracture danger, wrinkling occurrence and springback distortions.

The following step 1.3 within the uniform restraining forces approach aims to the Pareto front obtainment for the selected objective functions. The Pareto front provides all the possible compromise solutions: if the obtained scenario satisfies the design requirements, the procedure can be stopped, otherwise a spatially differentiated restraining force policy is developed in order to improve the current solutions. In such case the differentiation policy requires different attempts in order to verify if a localized control of the restraining forces can improve the current solutions. These choices are surely driven by the output obtained in step 1.2 and by designer experience. Moreover, phase 1 is essential before a differentiation in restraining forces is applied, since, when a complex sheet stamping process is designed, a preliminary analysis of material flow is necessary to define the sheet regions which are more critical in terms of defects localisation.

2.3 Phase 2

Once the analysis with a uniform restraining force was developed, phase 2 aims to improve the current solution. As far as step 2.1 is regarded, differentiated restraining forces depend on draw beads positioning and penetration and/or on the number of segments of the blank holder, as well as on the forces they apply. Therefore, the first issue to be accomplished, when differentiated restraining forces are chosen, is to individuate the right strategy of differentiation: how many draw beads? What are the best positions of the draw beads? Where do their actions have to be most relevant? If a segmented blank holder strategy is chosen: how many segments? The above questions have to be answered before implementing any optimization technique: an early knowledge of critical material flow regions in terms of thinning or springback etc. is unavoidable. In other words, step 2.1 allows to divide the stamped part in different zones each characterized by similar restraining forces values; in this way, it will be possible to control locally the restraining forces. It is worth pointing out, that if this knowledge is not available, the designer should proceed, for instance, by surrounding the blank profile by several and different draw beads; as a consequence, the number of variables to be optimized would increase dramatically and the subsequent optimization (step 2.2) could become very time consuming and difficult to manage.

Finally, step 2.2 is related to the application of a multi-objective (or mono-objective depending on the particular conditions) optimization methodology in order to select the best process parameters configuration (to optimise restraining forces).

In this paper, two case studies are presented: in the former case, step 2.2 was developed using a multi-objective approach, in the latter instead a mono-objective constrained minimization coupled with a MLS approximation was utilized to reach the final optimal solution. In particular, it was a constrained optimisation problem presenting a constraint on sheet draw-in. In the following some brief remarks on the general formulation of both multi-objective optimization

by Pareto optimal solutions search techniques and Moving Least Squares approximation are given.

2.4 Multi-objective optimization by Pareto optimal solutions search techniques

In order to implement a multi-objective approach, the following steps have to be developed.

- Modelling step including variables definition and identification of the different objective functions;
- Planning of the numerical simulations to be run through a proper Design of experiments (DOE) definition;
- Numerical simulations development according to the designed DOE;
- Collection of numerical data of objective functions for each of the conditions identified by the DOE;
- Meta-modelling step consisting in the analytical formulation of a response surface describing each objective function as a function of the design variables;
- Application of a multi objective optimization (for instance ε -constraint procedure) in order to determine optimal Pareto solutions.

A Pareto optimal solution is a solution which guarantees that, moving from it, no improvement can be obtained on one objective function without worsening any other goal (Deb 2001). Thus, the Pareto optimal solutions are compromises determined in the domain of the feasible solutions. There are many possibilities to find out the Pareto optimal solutions such as the sum weighted method and the ε -constraint methodology, Normal Boundary Intersection method (Das and Dennis 1997), the physical programming (Messac and Mattson 2002) just to mention some possibilities. Some authors (Das and Dennis 1997) showed that, when sum weights method is applied an even spread of the weights does not necessary result in an even distribution of the points in the Pareto set. Moreover, the spread of the points strongly depends on the relative scaling of the objectives. These authors suggest that drawbacks of sum weight methods enhance with the increasing of the number of the objectives to be managed and different approaches are proposed to overcome the aforementioned drawbacks, such as the Normal Boundary Intersection (NBI) (Das and Dennis 1997) method or the physical programming (PP) (Messac and Mattson 2002) one. Actually, in the cases investigated in this paper, an integration between the sum weight method and the ε -constraint methodology was enough to obtain a uniform distribution of the Pareto solutions all along the Pareto curve.

2.5 Moving Least Squares approximation

When a design strategy is implemented for stamping processes a certain number of direct problems have to be solved by numerical simulations. Often, the simulation time is very high and thus, the phenomenon behaviour is generally approximated by the well known surrogate models, also known as meta-models.

There are different methods able to carry out meta-models: some authors compared four popular meta-modelling techniques (polynomial regression, multivariate adaptive regression splines, radial basis functions and kriging) basing on multiple performance criteria (14 test problems representing different classes of problems were utilised) (Jin et al. 2001). The authors investigate the advantages and disadvantages of these four meta-modelling techniques: the most interesting conclusion is that there is not a unique meta-modelling technique suitable for every problem; actually, the performances depend on sample size and on the non-linearity order of the approximation function.

A contribution on the statistical methodologies for meta-models building when deterministic numerical simulation is utilized, is reported in Simpson et al. (2001). In this work a deep review of several techniques, including design of experiments, response surface methodology, Taguchi methods, neural networks, inductive learning and Kriging, is reported. Also, guidelines able to drive the designer towards the correct meta-modelling choice to implement are reported.

The optimization problems presented in this research do not present criticality in the RSM application. Response surface methods consist in the approximation of a given objective function to be optimised basing on a properly defined set of points belonging to the domain of variation of the independent variables the function itself depends on. The effectiveness of a RSM depends both on the proper definition of the Design of Experiments (DoE) and on the accuracy of function approximation. A very interesting aspect in RSM application regards the possibility to build response surfaces based on moving least squares approximations by utilising a moving region of interest. The MLS approximation is generally considered a performing as local approximation; this means that the MLS approach better approximates the region closer to the one chosen as reference point, actually, it is utilized when irregular grids of data have to be managed giving advantages in terms of approximation flexibility (Breitkopf et al. 2004, 2005).

In this paper, an advanced response surface methodology based on Moving least squares approximation technique is proposed. For the mono-objective case study.

The MLS approach works, starting from a proper DOE, as follows:

1. The approximated objective function $\bar{f}(\mathbf{x})$ can be defined through a basis function and proper coefficients according to the following polynomial expression:

$$\bar{f}(\mathbf{x}) = p^T(\mathbf{x}) a(\mathbf{x}) \tag{1}$$

2. The basis function $p(\mathbf{x})$ can be defined as consisting of linear and quadratic monomials:

$$p(\mathbf{x}) = \left\langle 1 \ x_1 \cdots x_n \ x_1 x_2 \cdots x_i x_{i+1} \cdots \frac{x_1^2}{2} \cdots \frac{x_n^2}{2} \right\rangle^T \tag{2}$$

where $x_1 \dots x_n$ are the components of vector \mathbf{x} .

3. Coefficients $a(\mathbf{x})$ can be obtained by minimizing the error $E(a)$ between experimental and approximated values of the objective function which, according to the weighted least squares method, can be expressed as:

$$E(a) = \sum_{j=1}^D w(\|\mathbf{x}_j - \mathbf{x}\|) \times \left(p^T(\mathbf{x}_j - \mathbf{x}) a(\mathbf{x}) - f(\mathbf{x}_j) \right)^2 \tag{3}$$

with D indicating the number of experiments/simulations belonging to the defined DOE;

4. Minimizing the error $E(a)$ provides:

$$a(\mathbf{x}) = A^{-1} B f \tag{4}$$

where

$$A = P W P^T; \ B = P W$$

with

$$P [\dots p(\mathbf{x}_j - \mathbf{x}) \dots]$$

and

$$W = \begin{bmatrix} w(\mathbf{x}_1 - \mathbf{x}) & & & 0 \\ & w(\mathbf{x}_2 - \mathbf{x}) & & \\ & & \ddots & \\ 0 & & & w(\mathbf{x}_D - \mathbf{x}) \end{bmatrix}$$

In the following sections the case studies will be presented and the results of the application of the proposed procedures will be discussed.

3 Case study A

3.1 Process description

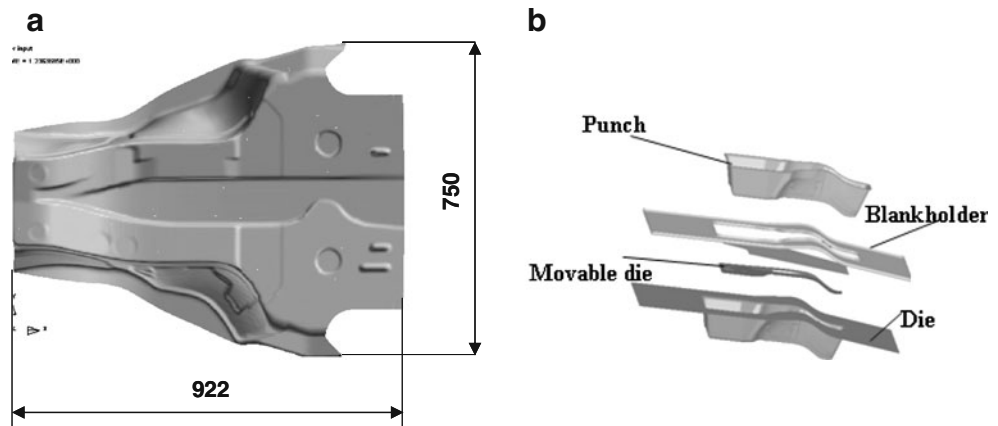
The first case study refers to the stamping process of a structural part from an automotive industrial production. The component material was ZSTE 300 BH steel characterized by yield strength of 380 MPa. Material flow rule (obtained through a campaign of tensile tests developed on 0° direction specimens) is reported in (5) while Lankford’s anisotropy parameters are: $r_{0^\circ} = 1,080$; $r_{45^\circ} = 1$; $r_{90^\circ} = 1,40$.

$$\sigma = 700 (\bar{\epsilon})^{0,16} \tag{5}$$

Geometrical features of the component are reported in Fig. 2 (sheet metal initial thickness was 1.6 mm) together with the tooling sketch.

The stamping operation follows different steps: the blank holder is first moved to clamp the blank, then punch let the blank reach the movable die surface and a coining phase

Fig. 2 The investigated component (dimensions in mm) (a) and tooling sketch (b)



occurs. Finally, the punch is moved deforming the sheet into the die cavity; in this phase the movable dies is moved steadily to the punch and applies a force of 250 [kN].

LS-Dyna explicit commercial code was utilized in order to simulate the proposed case study. The code takes into account the springback phenomena following a hybrid approach based on the explicit loading-implicit unloading analysis of the process. The utilized material has been modelled through the Barlat–Lian yield criterion considering an isotropic hardening law. The blank was meshed through about 800 quadrilateral shell elements; a four level geometric remeshing strategy was applied, thus, the total number of elements at the end of the explicit step is higher than 40,000. This choice was driven by the will to obtain a correct stress and strain prediction also in the small geometrical details characterizing the final component shape.

One of the authors has previously developed some researches on springback numerical simulation accuracy at the varying of some relevant numerical parameters (Fratini et al. 2008); according to the obtained results, a full integrated quadrilateral shell element with seven integration points along the thickness was utilized. As far as the punch velocity is regarded an artificially increased value equal to 0.5 m/s was utilized, checking that the kinetic energy was below the 10% of the deformation work, in order to avoid any inertia effect. Frictional actions were considered through a Coulomb model with a coefficient equal to 0.12.

3.2 Phase 0 of the procedure

The considered part is characterized by open surfaces and a large amount of springback is obtained after removing the tools. In particular, an “opening” of the cross section is observed. This phenomenon has to be taken into account in the design phase. Actually, such geometry variations could determine problems in the positioning of the stamped part in the trimming dies, causing some additional costs due to reworking operations and repositioning or even making impossible the trimming operation itself.

Increasing stretching mechanics in the blank during the stamping processes would be useful in order to minimize springback; actually, stretching increase induces a greater plastic deformation thus reducing springback.

In other words, the restraining forces have to be increased in order to achieve proper stretching phenomena and, as a consequence, thinning tendency increases too. The restraining forces drive the stamping process, thus, the process design variables are related to them and, in particular, the variable chosen was the blank holder force (BHF[kN]). The process mechanics led to select thinning tendency and springback occurrence as objective functions; the indicators utilised for such objectives are detailed in the following sections.

3.3 Phase 1 of the procedure

3.3.1 Step 1.1

The first phase of the procedure concerns the hypothesis of uniform restraining forces action. Step 1.1 of the design procedure (mapping of the process) was developed at the varying of the blank holder force (BHF). For each investigated condition the BHF value was kept constant all along the process duration. The different values of BHF utilised in the mapping step vary from 500 [kN] to 1,700 [kN].

3.3.2 Step 1.2

The springback amount and the thinning in the stamped part were collected at the end of each simulation.

The indicator chosen for thinning objective was the percentage value of maximum thinning indicated with $t\%$ in the following. As springback is concerned, it has to be noticed that after the implicit springback simulation, three sections of the part were considered (see Fig. 3) and, for each section, the angular deviation with respect to a reference geometry was measured.

For each section two angles were considered to measure the springback effect: the comparison between the obtained angle (α_o) and the desired one (α_d) was performed. The following indicator (Dev°) was utilized to estimate the deviation for each section (see Fig. 4).

$$Dev^\circ = (\alpha_{o1} - \alpha_{d1}) + (\alpha_{o2} - \alpha_{d2}) \quad (6)$$

Finally, due to the fact that section AA' presented the higher amount of springback distortions the value of Dev° at this

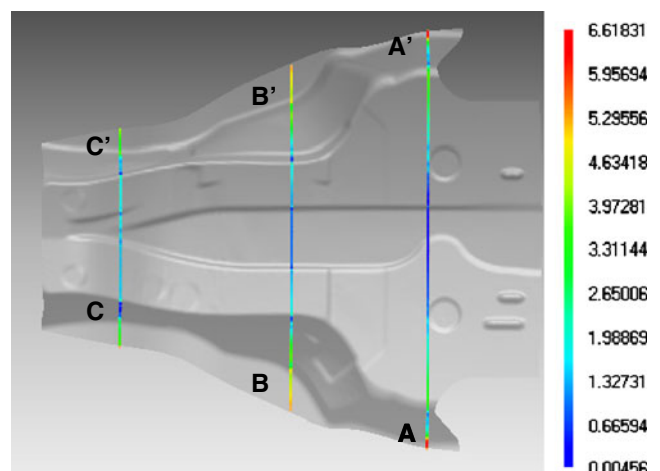
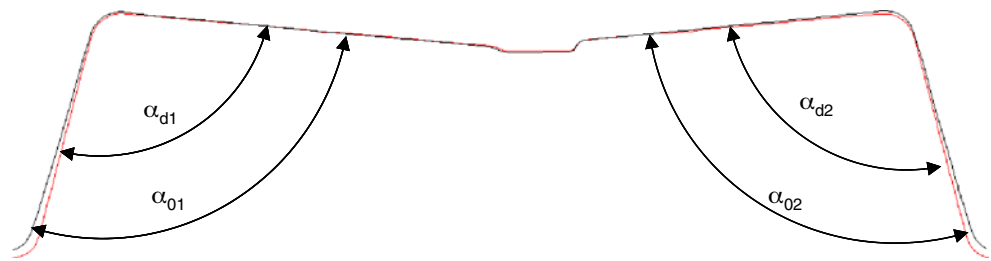


Fig. 3 Sections for springback measurement (distribution of the normal distances (mm) between the reference shape and the obtained one in the three sections)

Fig. 4 Angles utilized to calculate Dev°



section was taken in to account as objective function related to springback occurrence.

In the following Table 1, $t\%$ and Dev° values are reported for all the developed numerical simulations.

3.3.3 Step 1.3

In step 1.3 of the design procedure, as already mentioned, the Pareto front at the varying of uniform restraining forces has to be built. Thus, following the optimization steps reported in Section 2.4, after the modelling of the investigated problem, the meta-modelling step was performed. The analytical formulation of the response consisted of the determination, by proper regression models, of two fitting curves describing each objective function as a function of BHF. The best performing fitting curves were obtained by subsequent exclusions of factors, which are statistically less significant. Such procedure was developed in order to maximize an indicator of predictive performances, namely the adjusted correlation ($Adj-R^2$) coefficient. The following equations were obtained (expressed with normalized values of the input and output variables):

$$t\% = 0.33 + 2.83BHF - 8.4BHF^2 + 11.27BHF^3 - 5.16BHF^4 \tag{7}$$

$$Dev^\circ = 1.14 - 3.54BHF^2 + 2.85BHF^3 \tag{8}$$

Figure 5 summarizes the results of the Pareto analysis. Figure 5a reports the two best performing fitting curves (normalized values) for the two objective functions highlighting the conflicting trends of the two goals, both fitting curves present a monotonous behaviour at increasing of restraining forces: decreasing for springback and increasing for thinning. Therefore, a Pareto front was built: the Pareto

front results of prompt construction without using multi-objective methods as summing weighted scores method or ϵ -constraint. In fact, every $t\% - Dev^\circ$ couple corresponding to a particular BHF value is a Pareto solution: no solution exists that (for given operative conditions, i.e. for given BHF) for fixed thinning allows a lower springback. Figure 5b shows the obtained Pareto front, such curve is a very effective design tool: for instance, fixing a desired level of maximum thinning $t\%$, it is possible to foresee which minimum level of springback has to be expected. If a maximum thinning of 25% is admissible, the designer knows that the minimum obtainable springback (Dev°) is about 2° ; as well if a 30% of maximum thinning is acceptable, the designer has to expect a Dev° about 1° . Moreover, the Pareto front allows visualizing all the compromise solutions, making each design decision easier.

3.4 Phase 2 of the procedure

3.4.1 Step 2.1 Differentiating restraining forces

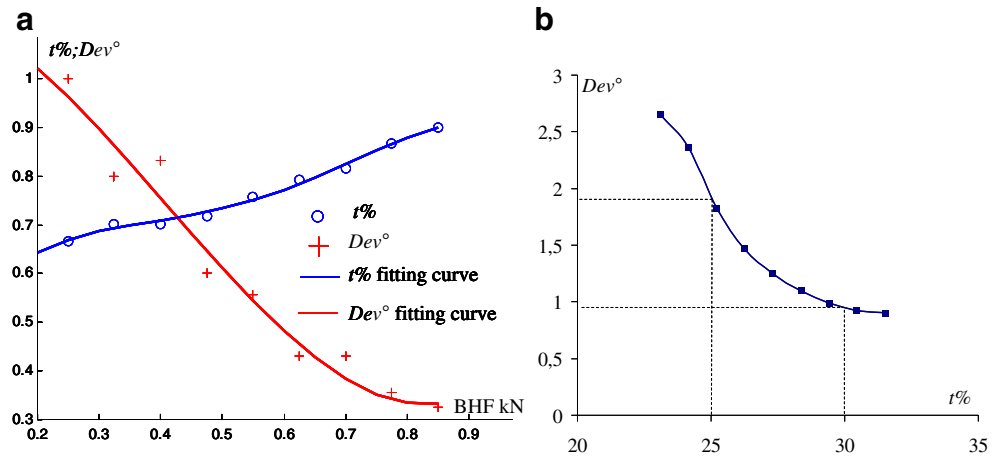
Analyzing the obtained results, it was possible to notice that the maximum thinning value and the maximum springback amount occurred in different regions of the final stamped part. In the following Fig. 6 the numerical results related to the simulations characterized by a BHF equal to 650 and 1,550 kN are, respectively, reported. As it can be observed, at the increasing of the blank holder force, the maximum thinning value increases too, but the maximum thinning zones remain the same all over the numerical simulations (Fig. 6a).

Moreover, in Fig. 6b the displacement due to springback occurrence, along the opening direction is reported; as it can be observed the maximum opening zone is localized close to the AA' section in both the simulations.

Table 1 Results of the numerical simulations

BHF [kN]	500	650	800	950	1,100	1,250	1,400	1,550	1,700
$t\%$	23.3	24.58	24.56	25.13	26.5	27.7	28.56	30.39	31.47
Dev°	2.68	2.14	2.23	1.61	1.49	1.15	1.15	0.95	0.87

Fig. 5 $t\%$ and Dev° fitting curves (a) and Pareto front (b)



It is clear that a localized increase of the restraining force in proximity of the section AA' could improve the solution in terms of springback amount without worsen

the maximum thinning value. Therefore, it is possible to divide the workpiece in different zones characterized by similar restraining force values, analyzing the results

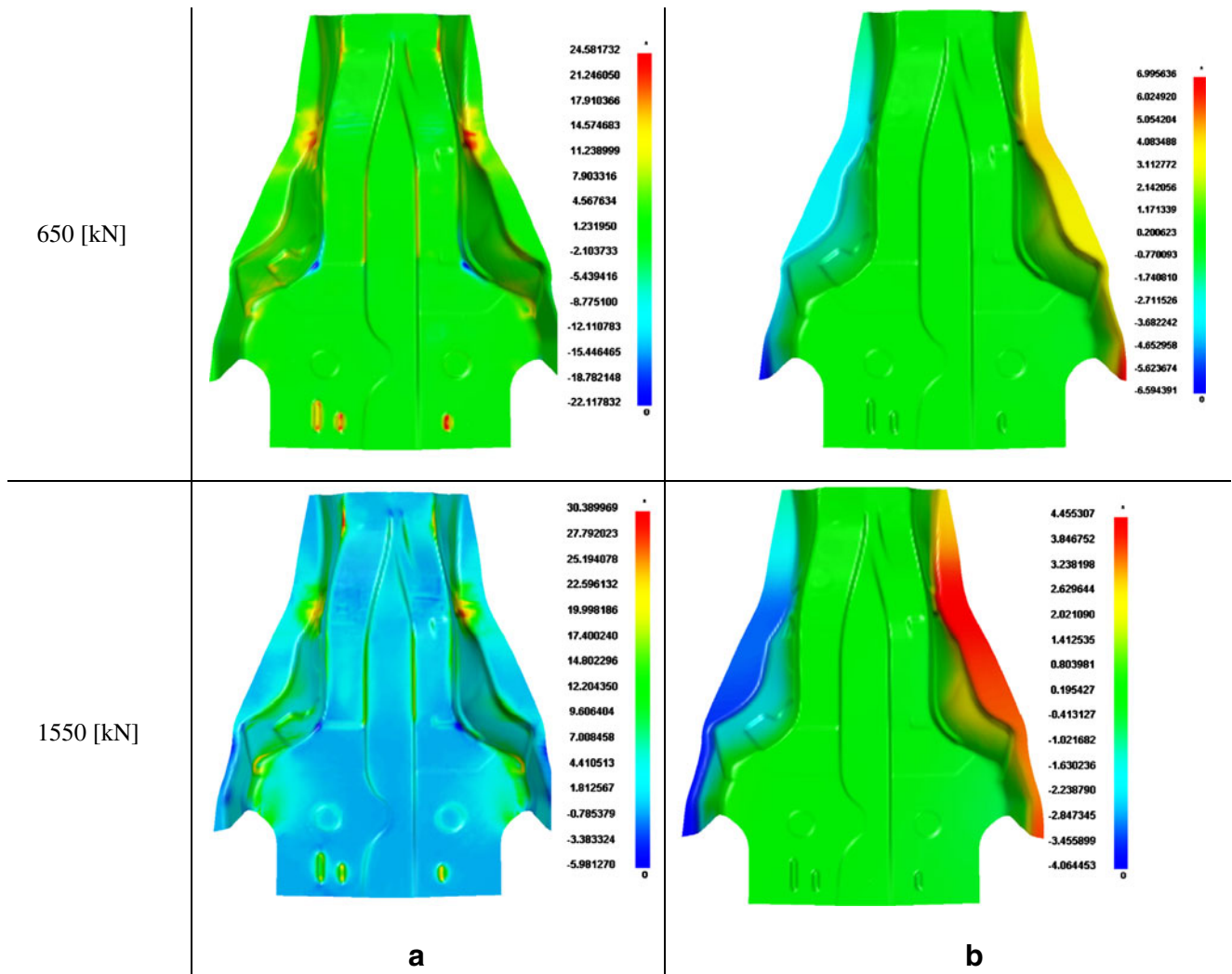


Fig. 6 Numerical results for BHF = 650 and 1,550 kN: thinning distribution (a) and springback distribution (b)

obtained in step 1.3. The proposed zones are evidenced in Fig. 7.

In order to evaluate and demonstrate that a differentiated restraining forces strategy can lead to better results, a first attempt utilizing draw beads action was developed. Region A is the area characterized by the maximum thinning value thus further restraining forces action should be avoided; on the contrary, a localized increase of the restraining force would be applied in region B, where a large amount of springback is obtained and no dangerous thinning is observed.

Therefore, the action of two draw beads placed upon region A was taken into account (in this numerical simulation a BHF equal to 950 kN was utilised). The numerical code permitted to model the draw beads through the introduction of equivalent restraining forces per unit length applied on the drawing blank. No geometrical effects of the utilized draw beads were considered.

The obtained solution led to very satisfactory results: in particular, a maximum thinning of about 25.5% and a Dev° equal to 0.5° were obtained. This result evidences that even if the thinning value is almost equal to the one shown in Table 1 (for BHF of 950 kN), the springback amount was strongly reduced (see again Table 1). The efficacy of the chosen technological solution can be demonstrated comparing the obtained results in terms of springback and maximum thinning, with the previously obtained Pareto front built with no draw beads action (see Fig. 8). As it can be observed point “DB₉₅₀” shows a strong improvement in terms of Pareto optimality.

It is worth pointing out that in this scenario, the Pareto front can be utilized as a sort of design support system identifying the correct directions of improvement for a more complete process engineering based on differentiated restraining forces optimization approach. Actually, the

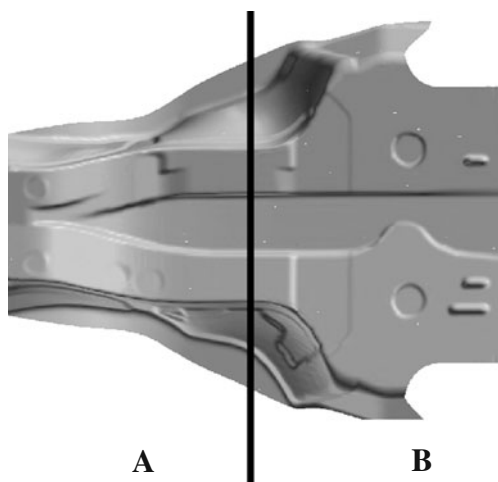


Fig. 7 Workpiece regions (a and b) identification

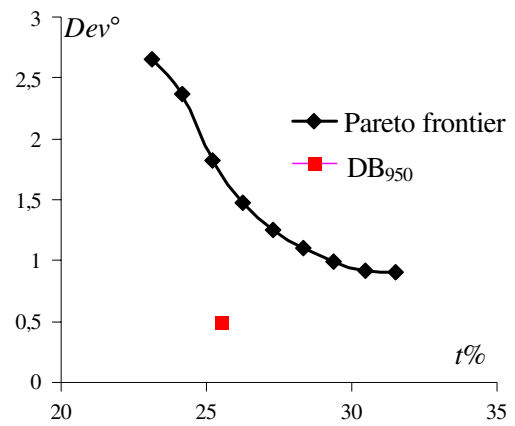


Fig. 8 Comparison between Pareto front and point DB₉₅₀

result illustrated in Fig. 8, proves that an optimization approach based on differentiated restraining forces would improve the final stamped part in terms of the monitored objective functions.

3.4.2 Step 2.2 Optimisation: multi-objective approach

Starting from the conclusions of the previous section, an optimization based on differentiated restraining forces policy was implemented. A multi objective approach was applied and the steps described in Section 2.4 were again developed. In this case two design variables were chosen: BHF and DBF which is the equivalent restraining force related to the draw beads action (force per unit length of draw beads). The deviation occurring in the section AA' was again taken into account as objective function related to springback occurrence (Dev°). On the contrary, as thinning is regarded, an index related to thickness distribution was utilized. This choice depends on the observation that the maximum thinning value $t\%$ depends only on the BHF value and it occurs in part regions far from the one over which draw beads act. Moreover, the draw beads action may induce localized thinning phenomena and therefore some localized thickening regions are present in the final component.

In order to control and minimize localized thickness variations, the thickness distribution, of two selected sections, was numerically extracted along a curvilinear distance (x_c). The chosen sections were placed where maximum thickening (Section 1) and maximum thinning (Section 2) were respectively observed (over the draw beads action area) as shown in Fig. 9.

As it should be observed in Fig. 9b, both localized thinning and thickening phenomena are evident. In particular, thickness distribution (T) was estimated by an indicator of the difference between the actual thickness t_i (at a given

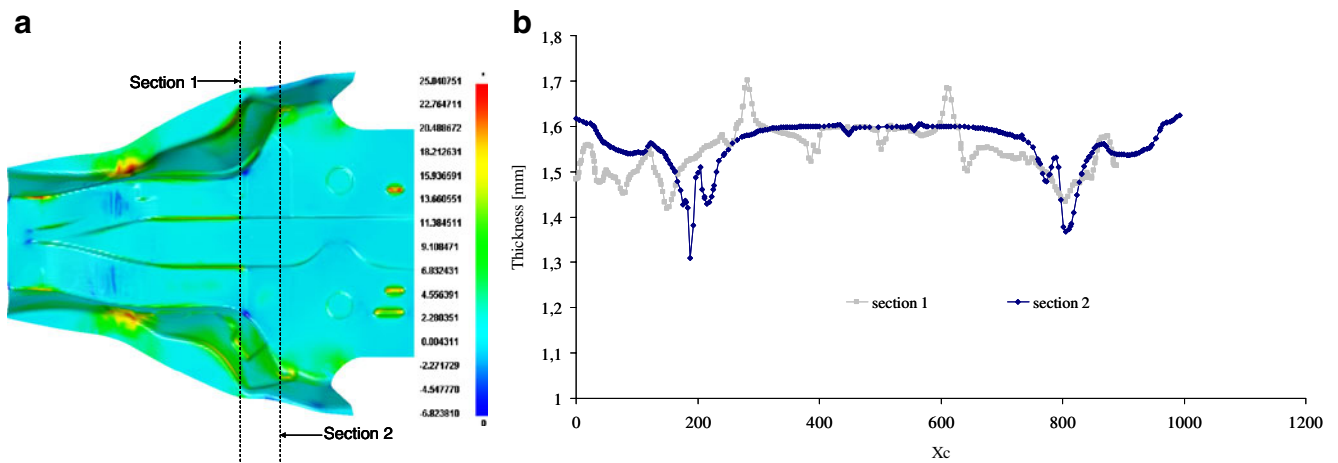


Fig. 9 Thinning map with sections 1 and 2 evidenced (a) and thickness along x_c (b)

value along the curvilinear distance x_c) and the initial thickness t_0 , as follows:

$$T = \sum_{x_c} \left(\frac{t_i}{t_0} - 1 \right)^2 \tag{9}$$

Once the new modelling phase was developed, the experiments were designed (i.e. the numerical simulations to be run). In particular, a regular five levels (for each design variable) DOE was designed in order to have a good approximation all over the variables domain.

The BHF range was fixed from 500 to 1,200 [kN] according to the results shown in Table 1. In this way, a maximum thinning of about 27% is reached in the numerical simulation characterized by the most critical restraining forces values. As the range of the equivalent restraining forces associated to the draw beads (DBF) action is regarded, it was selected with the aim to avoid that in AA' section a maximum thinning higher than 20% could occur. The

numerical simulations were developed and the objective functions values were extracted. Two response surfaces were obtained through a “heuristic” regression procedure (developed within Minitab Environment) by subsequent exclusions of factors, which are statistically less significant (Myers and Montgomery 2002). Such procedure led to third order polynomial functions for both the objectives providing very satisfying correlation indexes. Figure 10 shows the obtained response surfaces over the normalized variables space: conflicting evolutions of the objective functions is evident, therefore making crucial a multi-objective approach.

As it can be observed, the springback amount decreases with the increasing of the two variables values. As the thickness distribution surface is concerned, the surface is characterized by a sort of “channel”: actually, for low design variables values thickening arises in the final stamped part; on the contrary, for the highest restraining forces values localized thinning phenomena led to highest value of the T

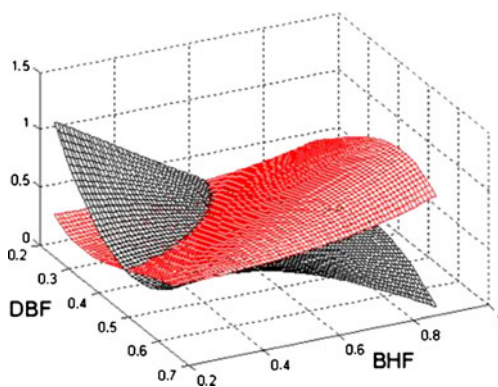


Fig. 10 Response surfaces for Dev° (black surface) and T (red surface)

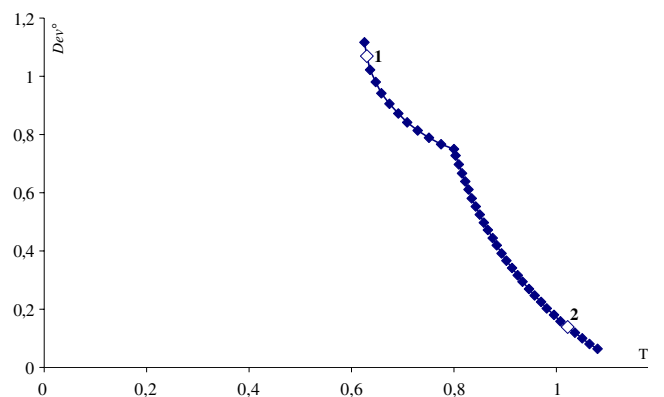
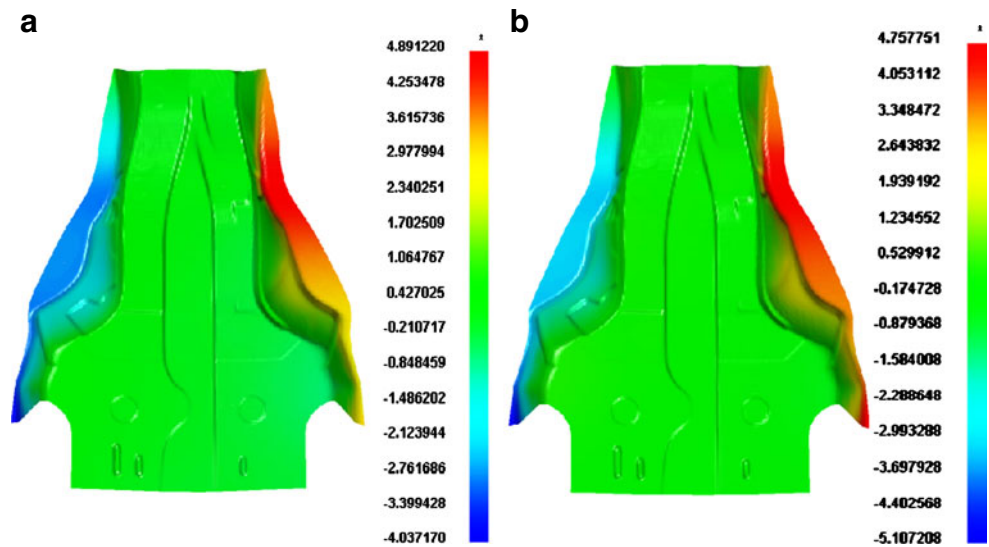


Fig. 11 Pareto front (Dev° vs. T)

Fig. 12 Springback distribution for solutions 1 (a) and 2 (b)



indicator. The Pareto optimal solutions can be determined by an ϵ -constraint procedure fixing Dev° function as primary function to be optimized. The resulting Pareto curve was determined and it is reported in Fig. 11 (curve Dev° vs. T). The non-convexity of the Pareto front fully justifies the ϵ -constraint method implementation.

In order to better explain the proposed tool effectiveness, two compromise Pareto solutions were selected and simulated (solutions 1 and 2 in Fig. 11): springback numerical results in terms of displacement along the opening direction are reported in the following Fig. 12 for the two selected solutions.

As it can be observed, moving from solution 1 to solution 2, springback amount decreases and a section opening reduction of about 1 mm is evident. Since the objectives are conflicting, thickness distribution will get worse moving from solution 1 to solution 2. Actually, in the following

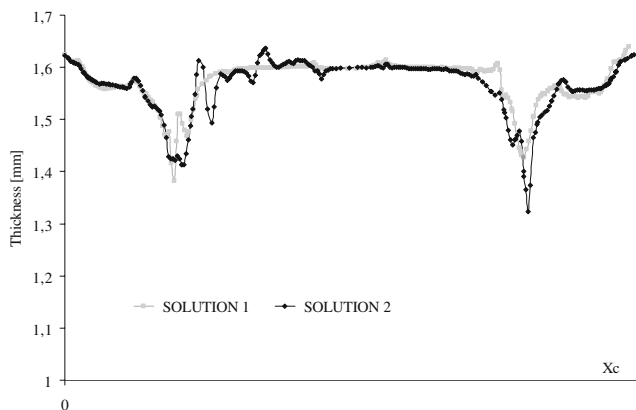


Fig. 13 Thickness distribution for solutions 1 and 2

Fig. 13, thickness distribution along section 1 is reported comparing solutions 1 and 2: Pareto solution 1 is characterized both by lowest thickness values and by less uniform thickness distribution.

To sum up, the obtained Pareto front enables to discriminate, for instance, which is the best possible T condition to be expected once a desired value of Dev° is fixed. In particular, it has to be noticed that a narrow range of T contains the optimal solutions space, and, moreover, Dev° values are strongly lower than the ones obtained in the Pareto front built with no draw beads action (see again Fig. 5b). Such result proves the effectiveness of the proposed approach and, what is more, the front provides the possibility to calibrate the design variables (DBF and BHF) in order to reach given levels of the chosen objectives.

4 Case study B

4.1 Remarks on MLS application

As already mentioned, in this second case study a mono-objective constrained minimization by MLS approximation was utilized to reach the final optimal solution (a constraint on sheet draw-in was taken into account). The implementation of a RSM approach utilizing a classic approximation based on least square error minimization (CA in the following) consists in a sequential application of the CA approximation over a zooming design space with an iterative optimum calculation. The procedure is summarized in Fig. 14 (\mathbf{x}_k indicates the design variables vector).

More in details, the dimensions of the design space are fixed thanks to the respect of technological limits on the

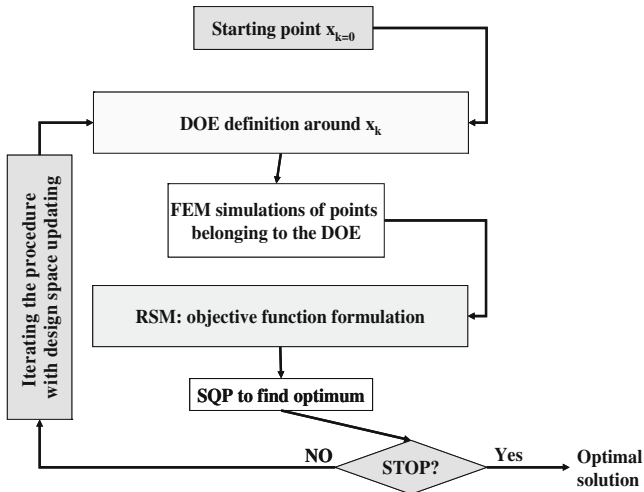


Fig. 14 Workflow of the optimization procedure

peculiar problem. On the explored design space, a RSM (based on the classical least squares approach) is utilized to approximate the response function for a chosen objective function ($f(\mathbf{x}_k)$) using a proper order approximation. The objective function is evaluated within the points belonging to this design space and its minimum is searched within the same space by a sequential quadratic programming (SQP) approach. A new DoE is built around the obtained minimum and the procedure is iterated up to reach the optimum. Figure 15 reports an example of DoE iterations in a design space with two variables x_1 and x_2 .

A novel approach based on MLS approximation consists of the following steps: firstly, a CA is performed over the starting DoE in order to identify the “optimum zone” i.e.

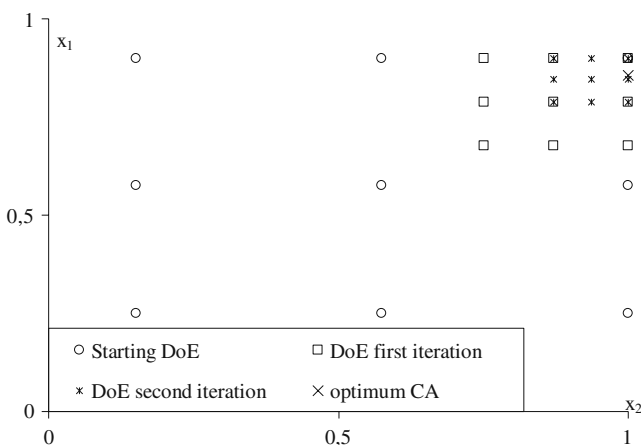


Fig. 15 Iterative DoE

the region over which the optimum has to be expected. Then, a sort of “progressive” application of the MLS is developed: the MLS approximation is applied over the whole design space (starting DoE) and using as reference point the one characterized by the lowest value of the objective function (indicated with M_1). Such application leads to a minimum indicated with M_2 . The progressive application of MLS using M_2 as reference point leads to a new minimum indicated with M_3 ; in other words, the procedure is iteratively developed.

Figure 16 illustrates an example of such iterative surfaces: response surfaces built with CA (red surface), MLS applied with respect to M_1 (green surface), MLS applied with respect to M_2 (black surface). The MLS approximations are not very performing in terms of prediction capabilities of the obtained response surfaces all over the whole domain, but offer better predictions for the points belonging to the neighbourhood of the optimum: the prediction errors limited to those points are significantly lower than the ones provided by CA. As it can be observed, the main effect is a better and smoother approximation moving from the red surface towards the black one in the optimum region. This means that by adding a single direct problem to the design space, a better approximation and a better minimum can be obtained. This results could be generalized foreseeing that in iterative applications of the procedure many numerical simulations could be avoided.

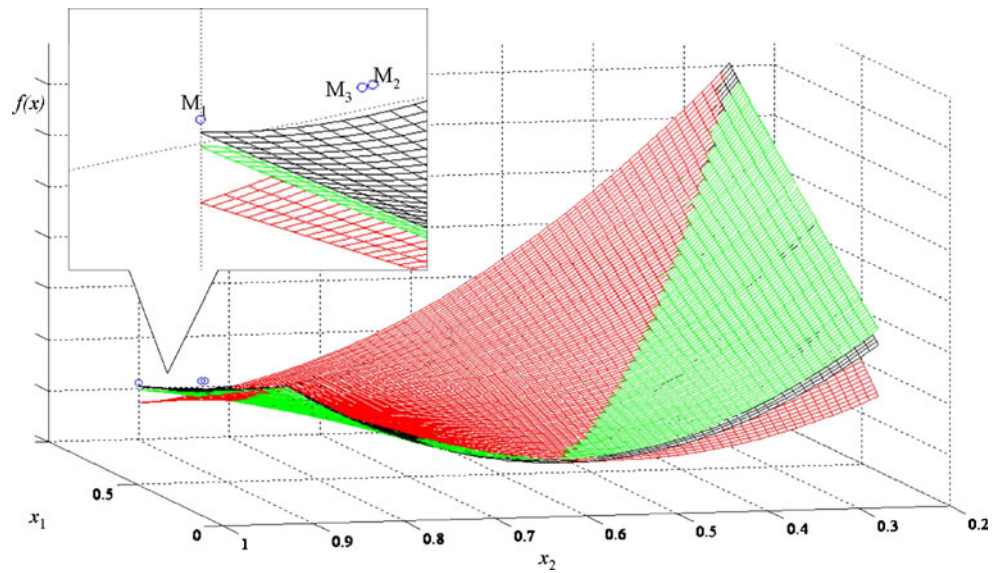
Within the application of the MLS it has to be highlighted that the weights of the expression (3) can be obtained by utilizing some weighting functions (Belytschko et al. 1996; Breikopf et al. 2004) well known from the literature.

It is easy to understand that the higher the weight associated to a point the more accurate the approximation of the surface for that point. The idea is to utilize this peculiarity and make the MLS approximation more flexible possible in order to reduce the computational effort of an optimization strategy. This aim is pursued by two policies: (a) instead of zooming the interest region implementing a new DoE it is possible to better approximate locally the objective function changing the reference point; (b) reuse of points already available within the design variables domain.

Moreover, once a certain optimum is reached (for instance the one indicated with M_3), the proposed approach allows to build a new response surface utilising such point and reusing some of the points already available from previous Designs of Experiments. Thus, the procedure may lead to a “final optimum” as the one illustrated in Fig. 15 by a low additional computational effort.

In Fig. 17 the better and smoother MLS approximation in the interest region is evident: the red surface was the one obtained by CA; the black one is the one obtained by MLS with respect to point M_3 . The main advantages of the proposed approach are a the better local approximation and a

Fig. 16 Comparison of the obtained response surfaces



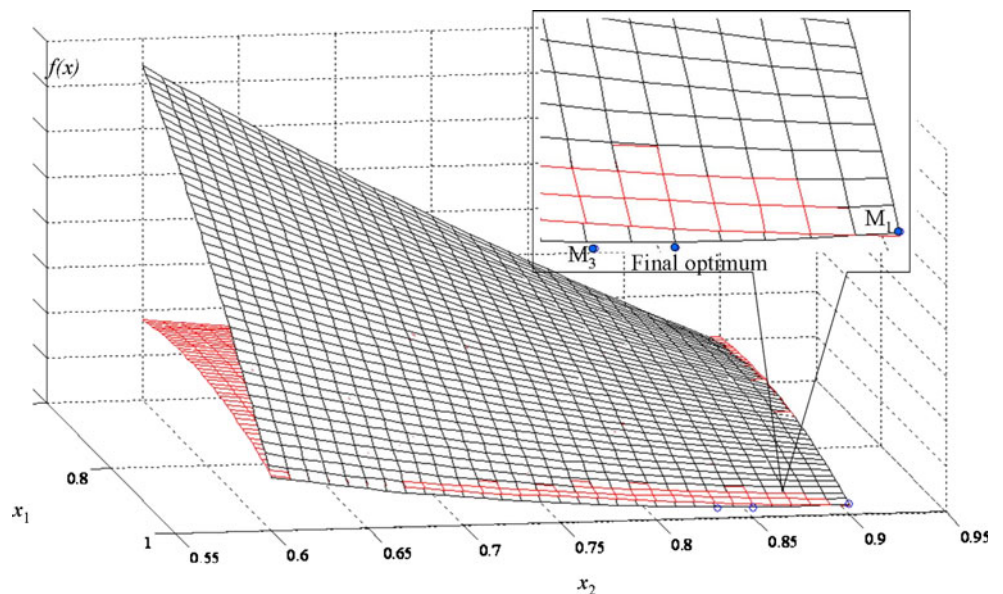
drastic reduction of the DoE points necessary to obtain a proper approximation in the interest region. These advantages can lead to a strong reduction of the computational effort in an iterative optimization procedure.

The proposed procedure can be summarized as follows:

1. Classical approximation based on least squares minimization on the whole domain in order to individuate the optimum zones.
2. Implementation of a MLS based approximation considering as reference point the best value of the DoE, as a consequence the new function better approximates the optimum region.
3. Minimization of the new function (minimum M_i).
4. MLS based approximation considering as reference point M_i .
5. Minimization of the new function (minimum M_{i+1}).
6. Checking: IF $M_{i+1} < M_i$ iterate the procedure ELSE go to 3.
7. Moving and zooming the interest domain utilizing reusing points policy.

The explained procedure perfectly fits for cases of unconstrained optimization: if a constraint has to be managed, the procedure can be applied as well. Of course, the approximation of the constraint has to be determined and the minimization of step 6 and 8 have to be managed as

Fig. 17 Final response surfaces



constrained researches. The same approximation used for the objective has to be utilized for the constraint. Actually, also for the constraint a global approximation in the beginning is useful as well as a progressive and more tuned approximation around the optimum region.

Another aspect concerns the size of the domain over which the optimum is searched; the size of the domain has to decrease with the zooming of the MLS based approximations. Actually, if a MLS approximation is utilized and the research domain contains also regions far from the reference point, the risk to find out false minimum is very high.

4.2 Process description

The considered component was a structural part from an automotive industrial production. Figure 18 shows the investigated component (punch length = 1,250 mm).

The sheet metal initial thickness was 1.2 mm and the material was AA6016 aluminium alloy characterized by the following flow rule obtained through a campaign of tensile tests developed on 0° (rolling) direction specimens:

$$\sigma = 422\varepsilon^{0.247} \tag{10}$$

the following Lankford's anisotropy parameters were determined: $r_{0^\circ} = 0,684$; $r_{45^\circ} = 0,555$; $r_{90^\circ} = 0,684$. The utilized material has been again modelled through the Barlat–Lian yield criterion considering an isotropic hardening law. The blank was meshed through quadrilateral shell elements; a four level geometric remeshing strategy was applied, thus, the total number of elements at the end of the explicit step is about 30,000. A full integrated quadrilateral shell element with seven integration points along the thickness was utilized. As far as the punch velocity is regarded an artificially increased value equal to 0.5 m/s was utilized and Frictional actions were considered through a Coulomb model with a coefficient equal to 0.12.

4.3 Phase 0 of the procedure

Three objectives were considered and collected at the end of each numerical simulation: the springback amount, the maximum thinning ($t\%$) and thinning distribution in the stamped part. Taking into account that in an industrial

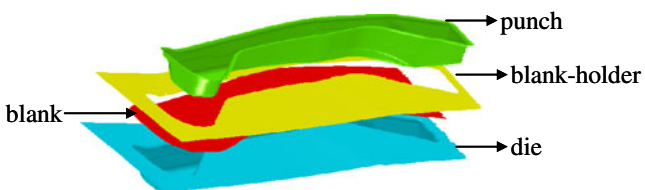


Fig. 18 Sketch of the industrial part

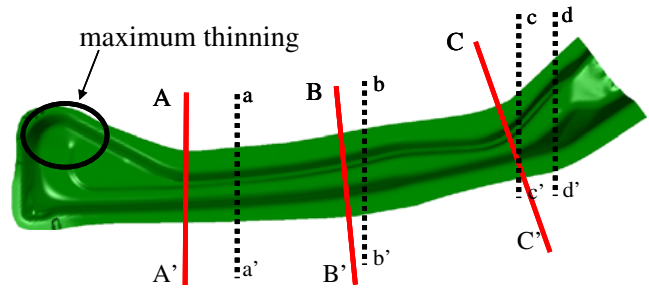


Fig. 19 Sections used to measure Dev° and d_{th}

environment a stamped part is evaluated also in terms of reached hardening, three different sections were chosen (AA', BB', CC' in Fig. 19) and the portion ($d_{th}[\text{mm}]$) of such sections reaching a fixed threshold for thinning (5%) was measured. After the implicit springback simulation, four sections of the part were considered (aa', bb', cc', dd' in Fig. 19) and, for each section, the angular deviation with respect to a reference part was measured obtaining a synthetic indicator (Dev°). Of course, the optimisation aims to maximise d_{th} while minimizing maximum thinning and springback. The design variable was the blank holder force (BHF):

4.4 Phase 1 of the procedure

4.4.1 Steps 1.1 and 1.2

In order to analyse the sensitivity of the stamping process to the blank holder force variations six simulations at the varying of BHF value in the range from 375 to 750 kN were carried out.

Three third degree equations were obtained by designing a proper DoE and applying a stepwise regression procedure: each equation represents the behaviour of $t\%$, Dev° and $d_{th}[\text{mm}]$ as functions of BHF. Figure 20 illustrates the evidence of springback effect in one of the analysed sections.

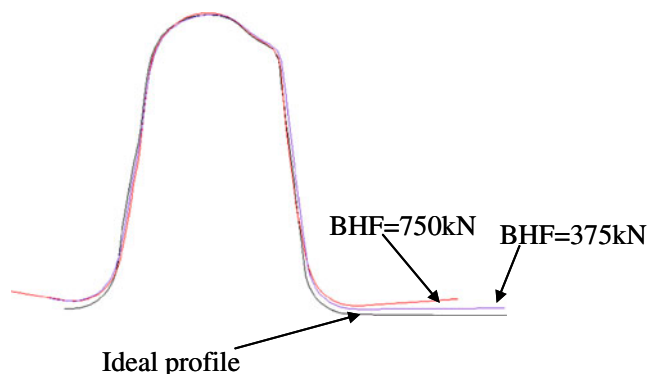


Fig. 20 Springback evidence in section aa'

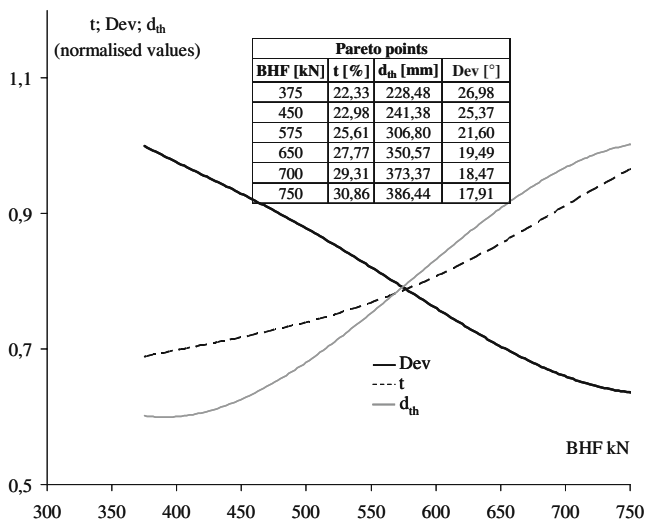


Fig. 21 Objective functions meta-models and Pareto points

4.4.2 Step 1.3

The application of the sum weight method led to the Pareto solutions for uniform BHF action; Fig. 21 illustrates the obtained curves (reporting normalised values of objective functions) together with the values of the three objective functions in some obtained Pareto points.

4.5 Phase 2 of the procedure

4.5.1 Step 2.1 Differentiating restraining forces

Once the numerical simulations with uniform restraining force were developed, step 2.1 has to be developed. For this issues the results of step 1.3 were again utilised to

find out the proper differentiation policy for the restraining forces. Figure 22 shows two solutions (thinning distributions) obtained with uniform BHF equal to 375 kN (a) and 750 kN (b) respectively, which are useful to explain the following differentiation policy.

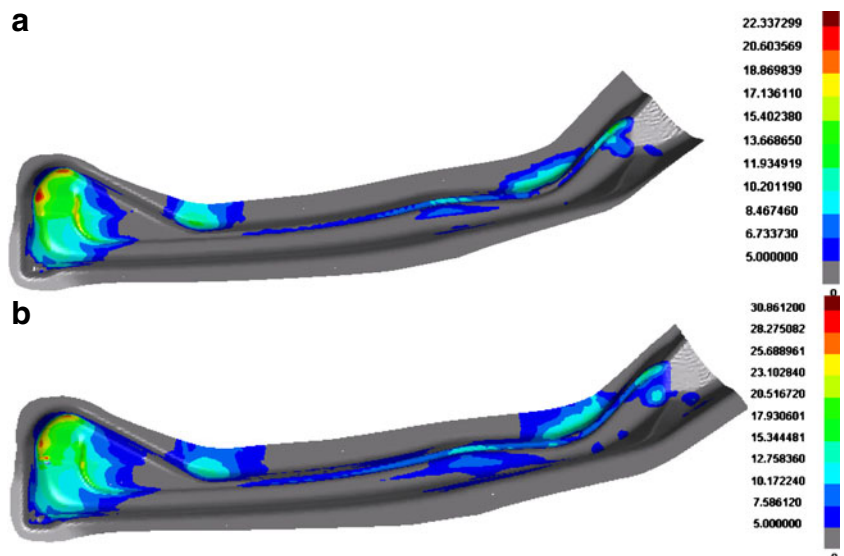
In particular, the material flow can be spatially differentiated in the three zones as shown in Fig. 23 since:

- Maximum thinning occurs in the region 1 all over the simulations: it is the zone characterised by a typical deep drawing mechanics, in this zone very low springback distortions are present;
- Springback is more evident region 2 and 3;
- Thinning distribution evidences that not enough hardening is obtained in zone 2, regions mainly characterised by bending actions.
- It is necessary to induce more stretching mechanics also in zone 3, but an excessive thinning value may occur due to the higher drawn height with respect to zone 2.

Therefore, the actions of some draw beads were taken into account; in particular, due to the above considerations, four draw beads were fixed in the positions illustrated in Fig. 24. Actually, the restraining forces actions were calibrated basing on the following assumptions:

- BHF was kept constant to a value of 375 kN which guaranteed the minimum value of t[%] (see again Fig. 21) when uniform restraining forces were applied;
- the variables to be optimised were DBF_i i.e. the equivalent restraining force related to the draw beads action (force per unit length of draw beads): actually, DBF₁ and DBF₂ were fixed in order to contain springback

Fig. 22 Thinning distributions obtained with uniform BHF equal to 375 kN (a) and 750 kN (b)



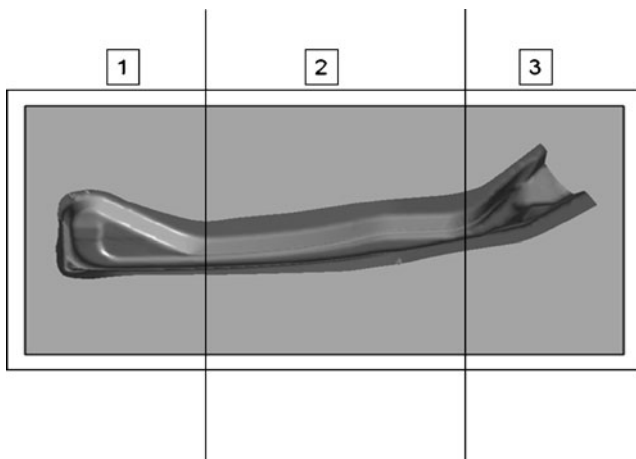


Fig. 23 Workpiece regions (1, 2 and 3) identification

- occurrence in their regions (and also due to the will to avoid excessive increasing of $t[\%]$);
- DBF_3 and DBF_4 became the variables to be optimised in order to reach enough hardening around sections AA' and BB' .

Moreover, as the latter issue is concerned, it has to be observed that the goal to increase d_{th} means that a stretching increase is necessary which also contributes to springback lessening, this hypothesis is further on confirmed analyzing again the Fig. 21 where the concordance of the two objectives is highlighted.

4.5.2 Step 2.2 Optimisation: mono-objective approach

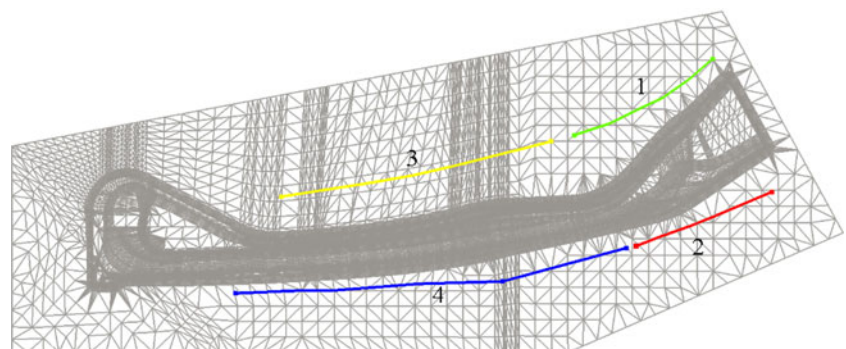
The investigated case study B does not require a multi-objective optimization since the objectives are not conflicting. Therefore the analysed problem can be managed as a mono-objective one with two design variables. The single objective to be accomplished is the maximization of $d_{th}[\text{mm}]$. Such maximization surely leads to an improvement of the current solution. The actions of DBF_3

and DBF_4 (design variables) have to be optimised and the corresponding necessary DoE has to be designed.

It is worth pointing out that the investigated stamping process is a very complex operation to manage. Actually, in such kind of processes the draw-in of the flange material is very sensitive to restraining forces variation; if a proper restraining force policy is not selected the material flow results unbalanced and heavy shape errors could be obtained in the final stamped part (see Fig. 25a). Moreover, in the analysed process it was observed that promising hardening results were possible even if the stamped part presents the aforementioned shape. These occurrences could make the optimization procedure ineffective. For these reasons, the numerical results evidenced the necessity to limit the draw-in determined by the draw beads actions in order to avoid geometrical errors on the final part. Therefore, a constraint was imposed within the optimisation problem limiting the draw-in value over the sheet profile. In particular, the minimum distances between the ideal profile and the obtained one after the stamping simulation was measured. This value can assume positive values (the flange is still present on both sides at the end of the stamping process) if the part was well stamped. Otherwise, it could assume negative values indicating that an excessive draw-in is present: the blank profile overcame the die fillet radius and, as a consequence, the stamped part does not satisfy the geometrical requirements (see Fig. 25b, segment c was measured to control the draw-in).

To sum up a mono-objective constrained optimisation with two variables was developed. The procedure illustrated in Section 4.1 was applied. As far as the constraint is regarded, the response surfaces were built following the same approximation peculiarity of the objective function. Furthermore, each minimization step was a constrained one. The application of the procedure consisted of two iterations: a central composite design (CCD) was used as starting DoE and 14 simulations were necessary to reach the final optimum (also thanks to the reusing points policy). The final optimal solution allowed the following values of the objective functions: $t\% = 22,37\%$; $Dev^\circ = 16,26^\circ$; $d_{th}[\text{mm}] =$

Fig. 24 Draw beads positioning



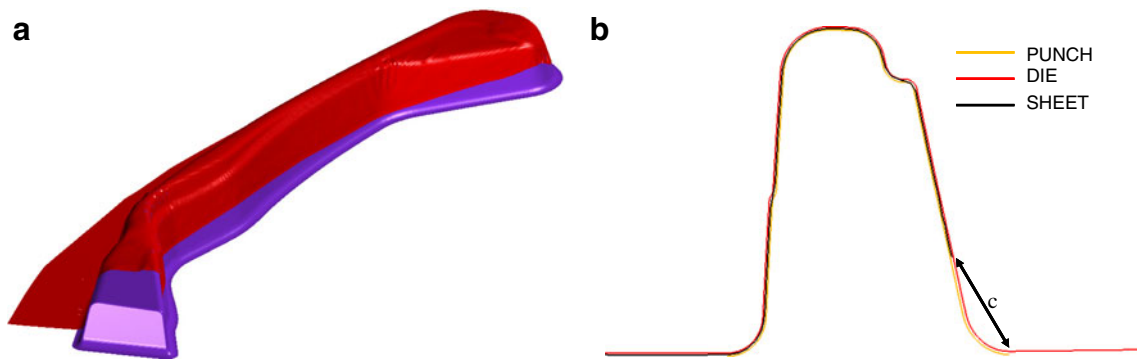


Fig. 25 Shape errors due to unbalanced material flow (a) and constraint control (b) by measure of segment c

536,41 mm. Figure 26 illustrates the numerical thinning map for the starting and the optimal solution.

As thinning distribution is concerned, a good result is obtained since the part regions controlled by DBF₃ and DBF₄ have largely reached the fixed threshold for thinning value. Actually, the final value of d_{th} is quite higher (better) than the ones reported in Fig. 21 for the Pareto points determined with uniform restraining forces. This major hardening also corresponds to a lower springback while maximum thinning remained around expected and acceptable values. Such results confirm that a proper differentiation in restraining forces is essential to accomplish conflicting goals.

It has to be pointed out that the above results were obtained fixing a BHF equal to 375 kN. As it can be noticed (see again Fig. 26) a large part of the stamped part is still

characterized by a thinning value lower than 5%. Thus the proposed solution can be surely improved, in particular additional restraining forces have to be applied. The draw beads action has been already optimized and higher values of their forces did not respect the draw-in constraint. Therefore, in order to increase the restraining forces and induce more hardening effect in the sheet the optimization procedure was again applied with a higher value of BHF. In particular, the same draw beads configuration shown in Fig. 24 was applied but with a BHF equal to 575 kN, this choice was driven by the will to induce more plastic deformation avoiding excessive thinning.

In fact, as shown in Fig. 21 the selected BHF value led to a maximum thinning of 25.6% that can be considered a proper threshold value in automotive sheet metal stamping field.

Fig. 26 Thinning map for uniform restraining force (BHF = 375 kN) (a) and for the optimal solution (b)

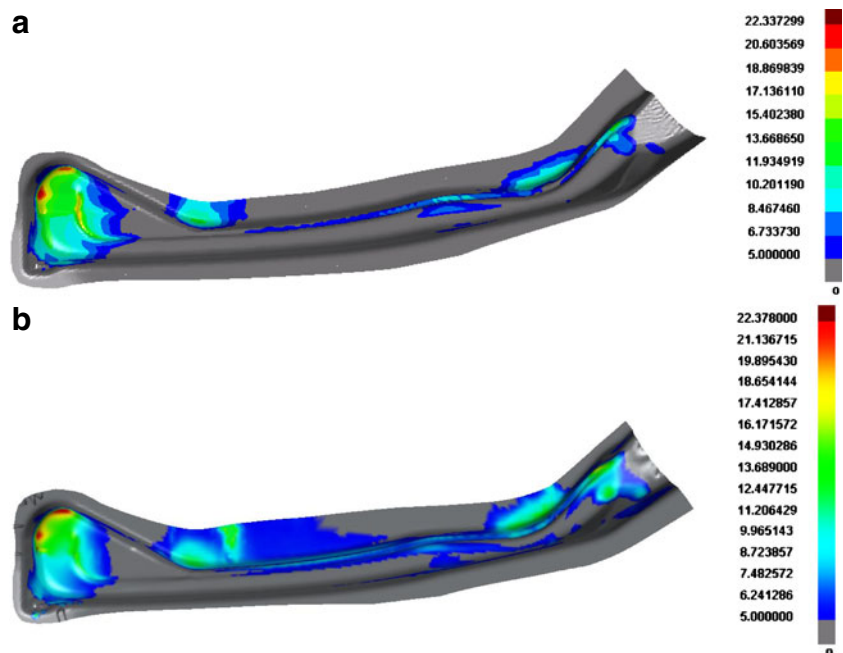
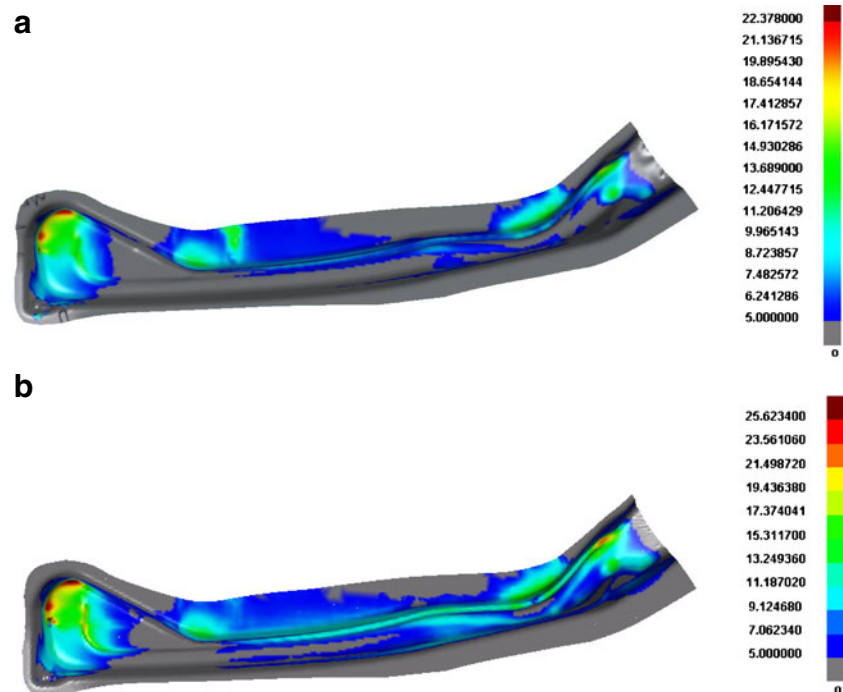


Fig. 27 Thinning map for the optimal solutions at BHF = 375 kN (a) and BHF = 575 kN (b)



The new optimum obtained in these conditions required a low computational effort. The comparison in terms of thinning distribution between the optimal solutions with BHF = 375 kN and BHF = 575 kN is reported in Fig. 27.

As it can be observed a significant improvement on d_{th} [mm] objective is reached with the respect to the optimal solution shown in Fig. 27 proving that a good calibration of restraining forces was developed. Moreover, this final solution shows good results also in terms of springback $Dev^\circ = 14.21^\circ$.

5 Conclusions

In this paper a contribution in terms of integration between FEM and computer aided optimisation techniques for stamping process design was presented.

The main goal of the paper was to provide an overview of the possibilities available to reach optimal design solutions: this goal was pursued by presenting some guidelines about the most suitable choices as optimisation tools are concerned.

The proposed guidelines were illustrated through the presentation of different case studies. In particular, the basic idea all over the proposed cases is that sheet stamping process optimisation problems are multi-objective ones and that such processes are governed by restraining forces.

Therefore, a policy based on spatially differentiated restraining forces was taken into account. The proposed pro-

cedure consists of a preliminary formulation of the investigated design problem (in terms of design variables and objective functions) and of two main phases: the former is focused on the problem contextualization with a uniform restraining force policy while the latter regards the differentiation of such forces. The proposed procedures always take into account springback as stamped part quality indicator.

A progressive design approach based on the integration of numerical simulations with optimization methodologies was presented. Response Surface Method, Moving Least Squares approximation and Pareto optimal solutions search techniques were applied in order to design two different complex 3D stamping operations. The proposed design methodology consisted of a former decision step leading to a Pareto front under the hypothesis of uniform restraining forces application. The following step was developed along two scenarios: a multi-objective approach or instead a mono-objective one.

In the former case study the optimization related to differentiated restraining force was developed by a multi-objective approach. The final Pareto front is a design tool which could be considered very effective also for industrial utilization: the Pareto curves can be used in order to discriminate which conditions have to be expected once a desired value of one the objective functions is fixed. In particular, it has to be noticed that such design tool allows choosing a desired value of one of the design objectives and provides the possibility to calibrate the design variables in order to reach a given level of the other objectives. To sum up a new

and flexible design methodology, able to cope with complex sheet metal stamping processes and to investigate many possible technological scenarios is proposed also providing a set of reliable solutions able to satisfy different design requirements.

The second case study, instead, deals with the mono-objective optimization approach, and in particular an innovative procedure is presented based on the application of a progressive moving least squares approximation.

The proposed methodology allows reducing computational effort: the progressive evolution allows reducing the design variables related to restraining force characterization. As a matter of facts the choice of draw beads number and positions is quick and straightforward. Moreover in the paper, an advanced optimization methodology, based on MLS approximation, focused on number of direct problems minimization, is also presented.

The paper aims to offer guidelines in computer aided optimization of complex sheet metal stamping processes, many scenario in terms of objective functions, design variables, optimization techniques are taken in to account, and an exhaustive range of sheet metal stamping issues is treated.

References

- Belytschko T, Krongauz Y, Organ D, Fleming M, Krysl P (1996) Meshless method: an overview and recent development. *Comput Met Appl Mech Eng* 139:3–47
- Breitkopf P, Rassineux A, Savignat PJM (2004) Integration constraint in diffuse element method. *Comput Methods Appl Mech Eng* 193:1203–1220
- Breitkopf P, Naceur H, Rassineux A, Villon P (2005) Moving least squares response surface approximation: formulation and metal forming applications. *Comput Struct* 83:1411–1428
- Castro C, Antonio C, Sousa L (2004) Optimisation of shape and process parameters in metal forging using genetic algorithms. *J Mater Process Technol* 146:356–364
- Cheng HS, Cao J, Xia ZC (2007) An accelerated springback compensation method. *Int J Mech Sci* 49:267–279
- Das I, Dennis JE (1997) A closer look at drawbacks of minimizing weighted sums of objectives for Pareto set generation in multicriteria optimization problems. *Struct Optim* 14:63–69
- Deb K (2001) *Multiobjective optimization using evolutionary algorithms*. Wiley, New York
- Di Lorenzo R, Ingarao G, Chinesta F (2009) A gradient-based decomposition approach to optimize pressure path and counterpunch action in Y-shaped tube hydroforming operations. *Int J Adv Manuf Technol* 44:44–60
- Di Lorenzo R, Ingarao G, Chinesta F (2010) Integration of gradient based and response surface methods to develop a cascade optimization strategy for y-shaped tube hydroforming process design. *Adv Eng Softw* 41:336–348
- Donglai W, Zhenshan C, Jun C (2008) Optimization and tolerance prediction of sheet metal forming process using response surface model. *Comput Mater Sci* 42:228–233
- Fann K, Hsiao P (2003) Optimization of loading conditions for tube hydroforming. *J Mater Process Technol* 140:520–524
- Fourment L, Do T, Habbal A, Bouzaiane (2005) A Gradient non gradient and hybrid algorithms for optimizing 2D and 3D forging sequences. In: *Proceeding of ESAFORM*, Cluj-Napoca, Romania
- Fratini L, Ingarao G, Micari F (2008) On the springback prediction in 3d sheet metal forming processes. *Steel Res International* 79:77–83
- Geng L, Wagoner RH (2004a) Die design method for sheet springback. *Int J Mech Sci* 66:1097–2003
- Geng R, Wagoner RH (2004b) Role of plastic anisotropy and its evolution on springback. *Int J Mech Sci* 44:123–128
- Hu W, Enying L, Li GY, Zhong ZH (2008) Optimization of sheet metal forming processes by the use of space mapping based meta-modelling method. *Int J Adv Manuf Technol* 39:642–655
- Ingarao G, Di Lorenzo R, Micari F (2009a) Analysis of stamping performances of dual phase steels: a multi-objective approach to reduce springback and thinning failure. *Mater Des* 30:4421–4433
- Ingarao G, Di Lorenzo R, Micari F (2009b) Internal pressure and counterpunch action design in Y-shaped tube hydroforming processes: a multi-objective optimisation approach. *Comput Struct* 87:591–602
- Jansson T, Andersson A, Nilsson L (2005a) Optimization of draw-in for an automotive sheet metal part. An evaluation using surrogate models and response surfaces. *J Mater Process Technol* 159:426–434
- Jansson T, Andersson A, Nilsson L (2005b) Optimization of draw-in for an automotive sheet metal part—an evaluation using surrogate models and response surfaces. *J Mater Process Technol* 159:234–426
- Jansson M, Nilsson L, Simonsson K (2007) On process parameter estimation for the tube hydroforming process. *J Mater Process Technol* 190:1–11
- Jin R, Chen W, Simpson TW (2001) Comparative studies of meta-modelling techniques under multiple modelling criteria. *Struct Multidisc Optim* 23:1–13
- Kazan R, Firat M, Tiryaki AE (2009) Prediction of springback in wipe-bending process of sheet metal using neural network. *Mater Des* 30:418–423
- Kleinermann J, Ponthot J (2003) Parameter identification and shape/process optimization in metal forming simulation. *J Mater Process Technol* 139:521–526
- Li K, Carden WP, Wagoner RH (2002) Simulation of springback. *Int J Mech Sci* 44:103–112
- Lin Z, Wang W, Chen G (2007) A new strategy to optimize variable blank holder force towards improving the forming limits of aluminium sheet metal forming. *J Mater Process Technol* 183:339–346
- Liu GP, Han X, Jiang C (2008) Novel multi-objective optimization method based on an approximation model management technique. *Comput Methods Appl Mech Eng* 197:2719–2731
- Meinders T, Burchitza IA, Bonte MHA, Lingbeek RA (2008) Numerical product design: springback prediction, compensation and optimization. *Int J Mach Tools Manuf* 48:499–514
- Messac A, Mattson CA (2002) Generating well-distributed sets of Pareto points for engineering design using physical programming. *Optim Engineering* 3:431–450
- Myers RH, Montgomery DC (2002) *Response surface methodology process and product optimization using designed experiments*, 2nd edn. Wiley, New York
- Naceur HA, Batoz J, Guo Y, Knopf-Lenoir C (2004) Optimization of draw bead restraining forces and draw bead design in sheet metal forming process. *J Mater Process Technol* 146:250–262
- Naceur H, Guo YQ, Ben-Elechi S (2006) Response surface methodology for design of sheet forming parameters to control springback effects. *Comput Struct* 84:1651–1663

- Naceur H, Ben-Elechi S, Batoz JL, Knopf-Lenoir C (2008) Response surface methodology for the rapid design of aluminium sheet metal forming parameters. *Mater Des* 29:781–790
- Oudjene M, Ben-Ayed L, Delameziere A, Batoz JL (2009) Shape optimisation of clinching tools using the response surface methodology with moving least-square approximation. *J Mater Process Technol* 209:289–296
- Pepelux L, Ponthot JP (2002) Finite element simulation of springback in sheet metal forming. *J Mater Process Technol* 125:785–791
- Rassineux A, Breilkopf P, Villon P (2003) Simultaneous surface and tetrahedron mesh adaptation using mesh free techniques. *Int J Numer Methods Eng* 57:371–389
- Schenk O, Hillmann M (2004) Optimal design of metal forming die surfaces with evolution strategies. *Comput Struct* 82:1695–1705
- Sheng Z, Jirathearanat S, Altan T (2004) Adaptive FEM simulation for prediction of variable blank holder force in conical cup drawing. *Int J Mach Tools Manuf* 44:487–494
- Shivpuri R, Zhang W (2009) Robust design of spatially distributed friction for reduced wrinkling and thinning failure in sheet drawing. *Mater Des* 30:2043–2055
- Simpson TW, Peplinski JD, Koch PN, Allen JK (2001) Meta-models for computer-based engineering design: survey and recommendations. *Eng Comput* 17:129–150
- Uthaisangsuk V, Prahl U, Bleck W (2007) Stress based failure criterion for formability characterisation of metastable steels. *Comput Mater Sci* 39:43–48
- Wagoner RH, Li M (2007) Simulation of springback: through-thickness integration. *Int J Plast* 23:345–360
- Wang L, Lee TC (2005) Controlled strain path forming process with space variant blank holder force using RSM method. *J Mater Process Technol* 167:447–455
- Wei L, Yuying Y (2007) Multi-objective optimization of an auto panel drawing die face design by mesh morphing. *Comput Aided Des* 39:863–879
- Wei L, Yuying Y (2008) Multi-objective optimization of sheet metal forming process using Pareto-based genetic algorithm. *J Mater Process Technol* 208:499–506
- Wei L, Yuying Y, Zhongwen X, Lihong Z (2009) Springback control of sheet metal forming based on the response-surface method and multi-objective genetic algorithm. *Mater Sci Eng A* 499:325–338
- Wu PD, Graf A, MacEwen SR, Lloyd DJ, Jain M, Neale KW (2005) On forming limit stress diagram analysis. *Int J Solid Struct* 42:2225–2241
- Xu WL, Ma CH, Li CH, Feng WJ (2004) Sensitive factors in springback simulation for sheet metal forming. *J Mater Process Technol* 151:217–222
- Zhang W, Shivpuri R (2009) Probabilistic design of aluminium sheet drawing for reduced risk of wrinkling and fracture. *Reliab Eng Syst Saf* 94:152–161
- Zhao G, Ma X, Zhao X, Grandhi R (2004) Studies on optimization of metal forming processes using sensitivity analysis methods. *J Mater Process Technol* 147:217–228